TABLE 10–4

Summary of expressions for laminar and turbulent boundary layers on a smooth flat plate aligned parallel to a uniform stream*

Property	Laminar	(a) Turbulent(†)	(b) Turbulent(‡)
Boundary layer thickness	$\frac{\delta}{x} = \frac{4.91}{\sqrt{\text{Re}_x}}$	$\frac{\delta}{x} \cong \frac{0.16}{(\text{Re}_x)^{1/7}}$	$\frac{\delta}{x} \cong \frac{0.38}{(\text{Re}_x)^{1/5}}$
Displacement thickness	$\frac{\delta^*}{x} = \frac{1.72}{\sqrt{\text{Re}_x}}$	$\frac{\delta^*}{x} \cong \frac{0.020}{(\text{Re}_x)^{1/7}}$	$\frac{\delta^*}{x} \cong \frac{0.048}{(\text{Re}_x)^{1/5}}$
Momentum thickness	$\frac{\theta}{x} = \frac{0.664}{\sqrt{\text{Re}_x}}$	$\frac{\theta}{x} \cong \frac{0.016}{(\text{Re}_x)^{1/7}}$	$\frac{\theta}{x} \cong \frac{0.037}{(\text{Re}_x)^{1/5}}$
Local skin friction coefficient	$C_{f,x} = \frac{0.664}{\sqrt{\text{Re}_x}}$	$C_{f,x} \cong \frac{0.027}{(\text{Re}_x)^{1/7}}$	$C_{f,x} \cong \frac{0.059}{(\text{Re}_x)^{1/5}}$

* Laminar values are exact and are listed to three significant digits, but turbulent values are listed to only two significant digits due to the large uncertainty affiliated with all turbulent flow fields.

† Obtained from one-seventh-power law.

‡ Obtained from one-seventh-power law combined with empirical data for turbulent flow through smooth pipes.

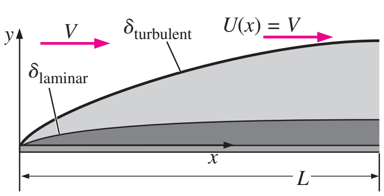

FIGURE 10–114
Comparison of laminar and turbulent boundary layers for flow of air over a flat plate for Example 10–12 (boundary layer thickness exaggerated).

EXAMPLE 10–12 Comparison of Laminar and Turbulent Boundary Layers

Air at 20°C flows at V = 10.0 m/s over a smooth flat plate of length L = 1.52 m (Fig. 10–114). (*a*) Plot and compare the laminar and turbulent boundary layer profiles in physical variables (u as a function of y) at $x = L$. (*b*) Compare the values of local skin friction coefficient for the two cases at $x = L$. (*c*) Plot and compare the growth of the laminar and turbulent boundary layers.

SOLUTION We are to compare laminar versus turbulent boundary layer profiles, local skin friction coefficient, and boundary layer thickness at the end of a flat plate.

Assumptions **1** The plate is smooth, and the free stream is calm and uniform. **2** The flow is steady in the mean. **3** The plate is infinitesimally thin and is aligned parallel to the free stream.

Properties The kinematic viscosity of air at 20°C is $\nu = 1.516 \times 10^{-5}$ m²/s.

Analysis (*a*) First we calculate the Reynolds number at $x = L$,

$$\text{Re}_x = \frac{Vx}{\nu} = \frac{(10.0 \text{ m/s})(1.52 \text{ m})}{1.516 \times 10^{-5} \text{ m}^2/\text{s}} = 1.00 \times 10^6$$

This value of Re_x is in the transitional region between laminar and turbulent, according to Fig. 10–81. Thus, a comparison between the laminar and turbulent velocity profiles is appropriate. For the laminar case, we multiply the y/δ values of Fig. 10–113 by δ_{laminar}, where

$$\delta_{\text{laminar}} = \frac{4.91x}{\sqrt{\text{Re}_x}} = \frac{4.91(1520 \text{ mm})}{\sqrt{1.00 \times 10^6}} = \mathbf{7.46 \text{ mm}} \quad (1)$$

This gives us y-values in units of mm. Similarly, we multiply the u/U values of Fig. 10–113 by U ($U = V = 10.0$ m/s) to obtain u in units of m/s. We plot the laminar boundary layer profile in physical variables in Fig. 10–115.

We calculate the turbulent boundary layer thickness at this same x-location using the equation provided in Table 10–4, column (a),

$$\delta_{\text{turbulent}} \cong \frac{0.16x}{(\text{Re}_x)^{1/7}} = \frac{0.16(1520\text{ mm})}{(1.00 \times 10^6)^{1/7}} = \mathbf{33.8\ mm} \qquad (2)$$

[The value of $\delta_{\text{turbulent}}$ based on column (b) of Table 10–4 is somewhat higher, namely 36.4 mm.] Comparing Eqs. 1 and 2, we see that the turbulent boundary layer is about 4.5 times thicker than the laminar boundary layer at a Reynolds number of 1.0×10^6. The turbulent boundary layer velocity profile of Eq. 10–82 is converted to physical variables and plotted in Fig. 10–115 for comparison with the laminar profile. The two most striking features of Fig. 10–115 are (1) the turbulent boundary layer is much thicker than the laminar one, and (2) the slope of u versus y near the wall is much steeper for the turbulent case. (Keep in mind, of course, that very close to the wall the one-seventh-power law does not adequately represent the actual turbulent boundary layer profile.)

(*b*) We use the expressions in Table 10–4 to compare the local skin friction coefficient for the two cases. For the laminar boundary layer,

$$C_{f,\,x,\,\text{laminar}} = \frac{0.664}{\sqrt{\text{Re}_x}} = \frac{0.664}{\sqrt{1.00 \times 10^6}} = \mathbf{6.64 \times 10^{-4}} \qquad (3)$$

and for the turbulent boundary layer, column (a),

$$C_{f,\,x,\,\text{turbulent}} \cong \frac{0.027}{(\text{Re}_x)^{1/7}} = \frac{0.027}{(1.00 \times 10^6)^{1/7}} = \mathbf{3.8 \times 10^{-3}} \qquad (4)$$

Comparing Eqs. 3 and 4, the turbulent skin friction value is more than five times larger than the laminar value. If we had used the other expression for turbulent skin friction coefficient, column (b) of Table 10–4, we would have obtained $C_{f,\,x,\,\text{turbulent}} = 3.7 \times 10^{-3}$, very close to the value calculated in Eq. 4.

(*c*) The turbulent calculation assumes that the boundary layer is turbulent from the beginning of the plate. In reality, there is a region of laminar flow, followed by a transition region, and then finally a turbulent region, as illustrated in Fig. 10–81. Nevertheless, it is interesting to compare how δ_{laminar} and $\delta_{\text{turbulent}}$ grow as functions of x for this flow, assuming either all laminar flow or all turbulent flow. Using the expressions in Table 10–4, both of these are plotted in Fig. 10–116 for comparison.

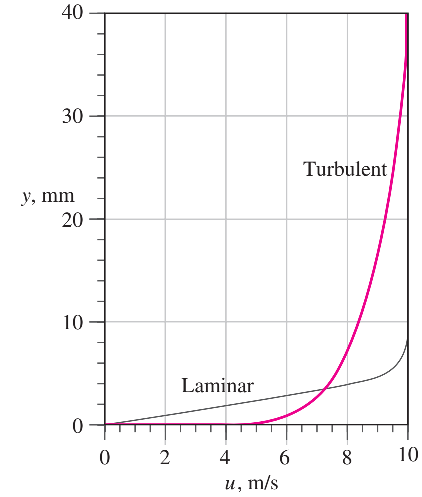

FIGURE 10–115
Comparison of laminar and turbulent flat plate boundary layer profiles in physical variables at the same x-location. The Reynolds number is $\text{Re}_x = 1.0 \times 10^6$.

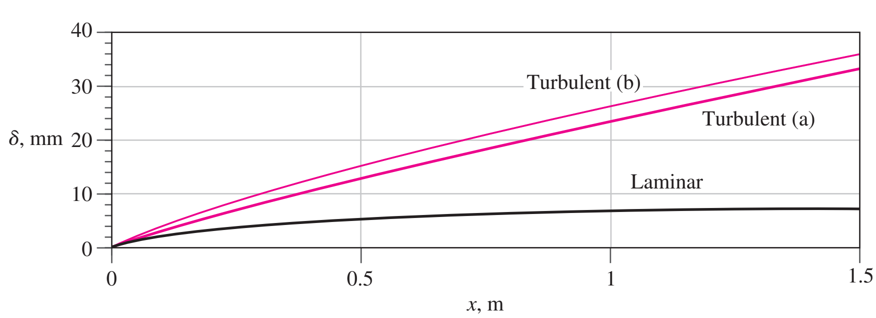

FIGURE 10–116
Comparison of the growth of a laminar boundary layer and a turbulent boundary layer for the flat plate of Example 10–12.

Discussion The ordinate in Fig. 10–116 is in mm, while the abscissa is in m for clarity—the boundary layer is incredibly thin, even for the turbulent case. The difference between the turbulent (a) and (b) cases (see Table 10–4) is explained by discrepancies between empirical curve fits and semi-empirical approximations used to obtain the expressions in Table 10–4. This reinforces our decision to report turbulent boundary layer values to at most two significant digits. The real value of δ will most likely lie somewhere between the laminar and turbulent values plotted in Fig. 10–116 since the Reynolds number by the end of the plate is within the transitional region.

The one-seventh-power law is not the only turbulent boundary layer approximation used by fluid mechanicians. Another common approximation is the **log law,** a semi-empirical expression that turns out to be valid not only for flat plate boundary layers but also for fully developed turbulent pipe flow velocity profiles (Chap. 8). In fact, the log law turns out to be applicable for nearly *all* wall-bounded turbulent boundary layers, not just flow over a flat plate. (This fortunate situation enables us to employ the log law approximation close to solid walls in computational fluid dynamics codes, as discussed in Chap. 15.) The log law is commonly expressed in variables nondimensionalized by a characteristic velocity called the **friction velocity** u_*. (Note that most authors use u^* instead of u_*. We use a subscript to distinguish u_*, a *dimensional* quantity, from u^*, which we use to indicate a nondimensional velocity.)

The log law:
$$\frac{u}{u_*} = \frac{1}{\kappa}\ln\frac{yu_*}{\nu} + B \qquad \textbf{(10–83)}$$

where

Friction velocity:
$$u_* = \sqrt{\frac{\tau_w}{\rho}} \qquad \textbf{(10–84)}$$

and κ and B are constants; their usual values are κ = 0.40 to 0.41 and B = 5.0 to 5.5. Unfortunately, the log law suffers from the fact that it does not work very close to the wall (ln 0 is undefined). It also deviates from experimental values close to the boundary layer edge. Nevertheless, Eq. 10–83 applies across nearly the entire turbulent flat plate boundary layer and is useful because it relates the velocity profile shape to the local value of wall shear stress through Eq. 10–84.

A clever expression that is valid all the way to the wall was created by D. B. Spalding in 1961 and is called **Spalding's law of the wall,**

$$\frac{yu_*}{\nu} = \frac{u}{u_*} + e^{-\kappa B}\left[e^{\kappa(u/u_*)} - 1 - \kappa(u/u_*) - \frac{[\kappa(u/u_*)]^2}{2} - \frac{[\kappa\,(u/u_*)]^3}{6}\right] \qquad \textbf{(10–85)}$$

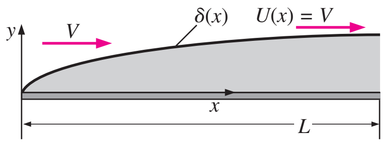

FIGURE 10–117
The turbulent boundary layer generated by flow of air over a flat plate for Example 10–13 (boundary layer thickness exaggerated).

EXAMPLE 10–13 Comparison of Turbulent Boundary Layer Profile Equations

Air at 20°C flows at V = 10.0 m/s over a smooth flat plate of length L = 15.2 m (Fig. 10–117). Plot the turbulent boundary layer profile in physical variables (u as a function of y) at $x = L$. Compare the profile generated by the